

RETRIEVAL AUGMENTED DIFFUSION MODEL FOR STRUCTURE-INFORMED ANTIBODY DESIGN AND OP- TIMIZATION

Anonymous authors

Paper under double-blind review

ABSTRACT

Antibodies are essential proteins responsible for immune responses in organisms, capable of specifically recognizing antigen molecules of pathogens. Recent advances in generative models have significantly enhanced rational antibody design. However, existing methods mainly create antibodies from scratch without template constraints, leading to model optimization challenges and unnatural sequences. To address these issues, we propose a retrieval-augmented diffusion framework, termed RADAb, for efficient antibody design. Our method leverages a set of structural homologous motifs that align with query structural constraints to guide the generative model in inversely optimizing antibodies according to desired design criteria. Specifically, we introduce a structure-informed retrieval mechanism that integrates these exemplar motifs with the input backbone through a novel dual-branch denoising module, utilizing both structural and evolutionary information. Additionally, we develop a conditional diffusion model that iteratively refines the optimization process by incorporating both global context and local evolutionary conditions. Our approach is agnostic to the choice of generative models. Empirical experiments demonstrate that our method achieves state-of-the-art performance in multiple antibody inverse folding and optimization tasks, offering a new perspective on biomolecular generative models.

1 INTRODUCTION

Antibodies, essential Y-shaped proteins in the immune system, are pivotal for recognizing and neutralizing specific pathogens known as antigens. This specificity primarily arises from the Complementarity Determining Regions (CDRs), which are crucial for binding affinity to antigens (Jones et al., 1986; Ewert et al., 2004; Xu & Davis, 2000; Akbar et al., 2021). The design of effective CDRs is therefore central to developing potent therapeutic antibodies, a dominant class of protein therapeutics. However, the development of these antibodies typically relies on labor-intensive experimental methods such as animal immunization or screening extensive antibody libraries, often failing to produce antibodies that target therapeutically relevant epitopes effectively. Thus, the ability to generate new antibodies with pre-defined biochemical properties *in silico* carries the promise of speeding up the drug design process.

Computational efforts in antibody design have traditionally involved grafting residues onto existing structures (Sormanni et al., 2015), sampling alternative native CDR loops to enhance affinities (Aguilar Rangel et al., 2022), and using tools like Rosetta for sequence design improvements in interacting regions (Adolf-Bryfogle et al., 2018). Many recent studies have focused on applying deep generative models to design antibodies (Luo et al., 2022; Martinkus et al., 2024; Zhu et al., 2024). They take advantage of geometric learning and generative models to capture the higher-order interactions among residues directly from the data. These innovations provide more efficient methods to search sequence and structure spaces.

Albeit powerful, current generative models struggle to design antibodies that adhere to structural constraints and exhibit desired biological properties. This challenge primarily arises from a lack of diversity in the available training data. Predominantly, research efforts have relied on the SAbDab database (Dunbar et al., 2014), which comprises fewer than ten thousand antigen-antibody complex

054 structures. The limited scope of this dataset restricts the models’ ability to capture comprehensive
 055 high-order interaction information between antigen-antibody residues, thereby increasing the risk of
 056 overfitting. Moreover, most existing methodologies attempt to design antibody sequences *de novo*,
 057 without the benefit of template-based guidance. This approach inherently demands a greater volume
 058 of data and extensive training or fine-tuning on specific datasets to achieve efficacy in practical
 059 applications.

060 In this work, we draw inspiration from
 061 template-based and fragment-based antibody
 062 design to develop a model that fully utilizes
 063 protein structural database, effective motif re-
 064 trieval, and semi-parametric generative neu-
 065 ral networks. Our goals are to: (a) leverage
 066 template-aware local and global protein geo-
 067 metric information to enhance model genera-
 068 tive capability, (b) integrate motif evolutionary
 069 signals to prevent overfitting, and (c) necessi-
 070 tate minimal training or fine-tuning for effective
 071 use in real-world applications.

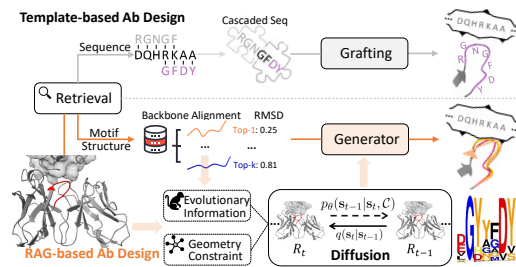


Figure 1: Illustration of the retrieval-augmented framework.

072 To this end, we introduce the **Retrieval-**
 073 **Augmented Diffusion Antibody** design model (RADAb), a novel semi-parametric antibody design
 074 framework. To fully exploit the protein structure space, we first compiled a database of CDR-like
 075 fragments from the non-redundant Protein Data Bank (PDB) (Berman et al., 2000). These CDR-like
 076 fragments are linear functional motifs structurally compatible with an antibody CDR loop, found in
 077 any protein geometry within the PDB. For a given antibody to be improved, we perform a structural
 078 retrieval to obtain motifs with structures similar to the desired CDR framework. As protein se-
 079 quences capable of folding into similar structures often share homology and consensus, we hypothe-
 080 size that these retrieved motifs, enriched with evolutionary information, can enhance the model’s
 081 generalization.

082 Unlike traditional rational design methods that optimize by grafting a single CDR fragment, we pro-
 083 pose to use a set of structural homologous CDR-like motifs together with the desired backbone for
 084 iterative sequence optimization (Figure 1). Our major contributions follow: (1) We propose a **first-**
 085 **of-its-kind** retrieval-augmented generative framework for rational antibody design. It uses a set of
 086 functional CDR-like fragments that satisfy the desired backbone structures and properties to guide
 087 generation toward satisfying all the required properties. (2) **A novel retrieval mechanism** is intro-
 088 duced for integrating these exemplar motifs with the input backbone through a novel dual-branch
 089 denoising module, utilizing both structural and evolutionary information. Additionally, we present a
 090 coupled conditional diffusion module that iteratively refines the evolution process by incorporating
 091 global and local conditions. This allows the model to incorporate more functional information than
 092 traditional antibody inverse folding models. (3) Empirical experiments demonstrate that our method
 093 improves the state-of-the-art methods in multiple antibody inverse folding tasks, e.g., an 8.08% AAR
 094 gains in long CDRH3 inverse folding task and an average of 7 cal/mol absolute $\Delta\Delta G$ improvements
 095 in functionality optimization task, offering a fresh perspective on biomolecular generative models.

096 **2 RELATED WORK**

097 **Antibody Design** Computational antibody design primarily follows two paths: conventional energy
 098 function optimization methods and machine learning approaches. Early antibody design methods
 099 were often limited to sequence similarity and energy function optimization (Lapidoth et al., 2015;
 100 Adolf-Bryfogle et al., 2018). Recent success of machine learning approaches mainly falls into two
 101 directions: antibody sequence design and antigen-specific antibody sequence-structure co-design.
 102 The methods used for antibody sequence design mainly include language-based models (Ruffolo
 103 et al., 2021; Olsen et al., 2022; Wang et al., 2023a) and inverse folding models (Dreyer et al., 2023;
 104 Høie et al., 2024). The other line focuses on antibody sequence-structure co-design mainly taking
 105 antibody-antigen complex as a graph, then using graph networks to extract features and predict the
 106 coordinates and residue type of antibody CDR (Jin et al., 2021; Kong et al., 2022; 2023; Lin et al.,
 107 2024; Luo et al., 2022; Zhu et al., 2024; Martinkus et al., 2024). **While these works are undoubt-**

108 edly powerful, they often generate antibodies from scratch without incorporating explicit structure
 109 constraints, which can introduce challenges in designing functional antibodies (Zhou et al., 2024).
 110 Instead, our method leverages the power of templates from a structure-informed perspective.

111 **Diffusion generative models** Diffusion models (Sohl-Dickstein et al., 2015; Song et al., 2020; Ho
 112 et al., 2020) are a class of generative models that have achieved impressive progress on a lot of
 113 generation tasks. Denoising diffusion probabilistic models (DDPMs) are a branch of diffusion mod-
 114 els, which contain two Markov processes. The forward process perturbs the data into pure noise,
 115 and then learns to generate data by reversing the forward Markov process. Because of the diffu-
 116 sion model’s flexibility and controllability, numerous works are focusing on employing retrieval-
 117 augmented methods to complement the diffusion framework for text-to-image generation (Sheynin
 118 et al., 2023), image generation (Blattmann et al., 2022), human motion generation (Zhang et al.,
 119 2023a) and small molecule generation (Huang et al., 2024).

121 **Retrieval augmented generative models** Retrieval augmented generation technique was first pro-
 122 posed in the field of natural language processing to enhance the language models by introducing an
 123 additional database (Lewis et al., 2020; Guu et al., 2020), prompting the language models to gen-
 124 erate more realistic and diverse results. Subsequently, retrieval augmented generation (RAG) has
 125 conducted diverse explorations in large fields, including natural language processing (Zhang et al.,
 126 2023b; Gao et al., 2023; Xu et al., 2024; Yoran et al., 2024; Caffagni et al., 2024) and computer
 127 vision (Long et al., 2022; Blattmann et al., 2022; Hu et al., 2023; Rao et al., 2023).

128 RetMol(Wang et al., 2023b) and IRDiff(Huang et al., 2024) are two retrieval-augmented small
 129 molecule generation models. RetMol generates new molecules based on existing small molecules
 130 by retrieving a set of exemplar moleculars, while IRDiff enhances protein-specific molecular gener-
 131 ation by using protein pockets to retrieve moleculars which interact with the pocket. Although there
 132 has been some retrieval work in the field of protein design and discovery (Zhou & Grigoryan, 2015;
 133 Aguilar Rangel et al., 2022), to the best of our knowledge, this is the first-of-its-kind retrieval-based
 134 generative framework for antibody design.

136 3 PRELIMINARIES AND NOTATIONS

138 3.1 NOTATIONS

140 Antibody consists of two heavy chains and two light chains. Each chain’s tip has a complementary
 141 site that specifically binds to a unique epitope on the antigen. This site includes six complementary-
 142 determining regions (CDRs): CDR-H1, CDR-H2, and CDR-H3 on the heavy chain, and CDR-L1,
 143 CDR-L2, and CDR-L3 on the light chain (Presta, 1992; Al-Lazikani et al., 1997).

144 Our work represents each single protein residue in terms of the residue type $s_i \in$
 145 $\{ACDEFGHIKLMNPQRSTVWY\}$, the coordinate $x_i \in \mathbb{R}^3$, and the orientation $\mathbf{O}_i \in$
 146 $\text{SO}(3)$, where $i = 1, \dots, N$ and N is the number of residues in the complex. Concretely, assuming the
 147 CDR sequence to be generated includes m amino acids and starts from position a , it can be denoted
 148 as $R = \{s_j \mid j \in \{a + 1, \dots, a + m\}\}$. Let M be the length of the antibody, the antibody frame-
 149 work is defined as $C_{ab} = \{(s_i, x_j, \mathbf{O}_j) \mid i \in \{1, \dots, M\} \setminus \{a + 1, \dots, a + m\}, j \in \{1, \dots, M\}\}$. The
 150 antibody framework sequence is defined as $S_{ab} = \{s_i \mid i \in \{1, \dots, M\} \setminus \{a + 1, \dots, a + m\}\}$. The
 151 antigen is defined as $C_{ag} = \{(s_i, x_i, \mathbf{O}_i) \mid i \in \{M + 1, \dots, N\}\}$. The retrieved CDR-like fragments
 152 are defined as $\mathbb{A} = \{A_i \mid i \in \{1, \dots, k\}\}$. The goal of our framework is to extract the antibody
 153 CDR structure from the antibody framework complex C_{ab} , then input it into the retrieval module to
 154 retrieve \mathbb{A} , and ultimately predict the distribution of R through C_{ag} , C_{ab} and \mathbb{A} .

156 3.2 DIFFUSION MODEL FOR ANTIBODY DESIGN

158 Due to diffusion models’ excellent performance and controllability, there are now many diffusion-
 159 based works that have achieved notable results (Luo et al., 2022; Villegas-Morcillo et al., 2023;
 160 Kulytė et al., 2024). To be specific, they are denoising probabilistic diffusion models that transform
 161 the amino acid type s , the backbone $C\alpha$ atom coordinates x , and the amino acid orientation \mathbf{O} during
 the diffusion process. We focus on sequence, of which the forward process perturbs the data in the

162
163
164
165
166
167
168
169
170
171
172
173
174
175
176
177
178
179
180
181
182
183
184
185
186
187
188
189
190
191
192
193
194
195
196
197
198
199
200
201
202
203
204
205
206
207
208
209
210
211
212
213
214
215

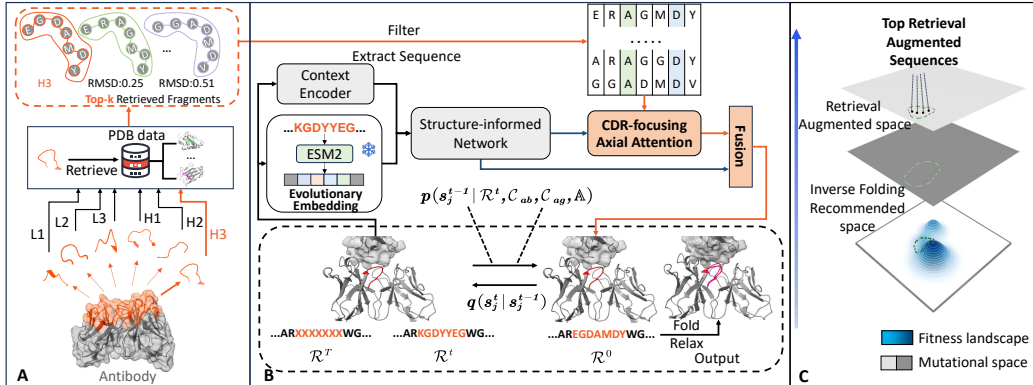


Figure 2: The overall architecture of the proposed RADAb framework. (A) Structural retrieval process, the CDR backbone is input into MASTER and the output is a set of ranked CDR-like fragments. (B) Diffusion process and denoising network which takes antibody-antigen context and retrieved evolutionary information as conditions. **The structure is fixed during diffusion process.** (C) Our method restricts the antibody to a small region through fixed structural constraints and retrieval-augmented constraints (functional constraints) to achieve higher fitness.

following ways (Hooigeboom et al., 2021):

$$q(s_j^t | s_j^{t-1}) = \text{Multinomial} \left((1 - \beta^t) \cdot \text{onehot}(s_j^{t-1}) + \beta^t \cdot \frac{1}{20} \cdot \mathbf{1} \right) \quad (1)$$

where β^t is the noise schedule for the diffusion process, as t approaches T , β^t will approach 1, and the probability distribution will become closer to pure noise. $\mathbf{1}$ corresponds to a 20-dimensional all-one vector.

To reverse the aforementioned forward process and denoise to generate CDR sequence, predictions need to be made by a neural network $F(\cdot)[j]$, which takes the antibody-antigen context as condition:

$$p(s_j^{t-1} | \mathcal{R}^t, C_{ab}, C_{ag}) = \text{Multinomial} (F(\mathcal{R}^t, C_{ab}, C_{ag})[j]) \quad (2)$$

As an example, this work uses Diffab (Luo et al., 2022) as the backbone for the generative model to conduct retrieval augmented generation. Note that the proposed retrieval system is generative model agnostic, and the developed modules can be integrated with any diffusion generative model.

4 METHODS

We propose RADAb (as demonstrated in Figure 2), a novel structure-informed retrieval-augmented diffusion framework for antibody sequence design and optimization. The model uses a structural retrieval algorithm to search for antibody homologous structures and take their sequences as conditional inputs for the diffusion model to provide homologous patterns and evolutionary information.

4.1 STRUCTURAL RETRIEVAL OF CDR FRAGMENTS

The structure of a protein is determined by its sequence, and protein sequences that can fold into similar structures exhibit similar properties. These structurally similar protein sequences contain rich evolutionary information. Based on this, we perform retrieval in the PDB database using CDR structures, aiming to obtain fragments that are similar to the real CDR and have homologous sequences, with the expectation that they possess similar functions.

To balance the quality of results and the retrieval speed, we use MASTER (Zhou & Grigoryan, 2015) for the search. MASTER uses the root-mean-square deviation (RMSD) of backbone atoms as a similarity measure. It queries structural fragments composed of one or more non-contiguous segments and can find all matching fragments from the database within a given RMSD threshold. This allows for fast and accurate searches in the PDB database for protein motifs. Note that MASTER

can utilize only the backbone information without any leakage of sequence data during the search process. The retrieval procedure is described in Algorithm 1 and detailed in Appendix A.3.

For the retrieved results, we use the RMSD with the real backbone structure as a score to rank them and filter out the input CDR fragment. For ease of use, we further constructed a CDR-like fragments database (detailed in Appendix A.4). Additionally, to enable the model to learn richer evolutionary information, we filter out identical CDR-like sequences during the training phase. However, to improve the quality of the model’s generation, we do not perform similar filters during generation.

Algorithm 1 Structural Retrieval Algorithm Overview

```

1: Input: Coordinates set  $\mathcal{X} = \{x_k \mid k \in \{1, \dots, m\}\}$ 
2: Input: Structure database with  $P$  structures  $\mathbb{T} = \{\tau_i \mid i \in \{1, \dots, P\}\}$ 
3: Initialize CDR-like fragments set:  $\mathbb{A} \leftarrow \emptyset$ 
4: Initialize structure residues set:  $\mathcal{C} \leftarrow \emptyset$ 
5: Initialize threshold  $\maxA()$ ,  $\maxB()$ ,  $\maxC()$ 
6: for  $i = 1$  to  $P$  do
7:    $\mathcal{C} \leftarrow$  all residues in  $\tau_i$ 
8:   for each residue  $j$  in  $\mathcal{C}$  do
9:      $r \leftarrow \text{RMSD}(\mathcal{X}, j)$ 
10:    if  $r > \maxA(\mathcal{X})$  then
11:      eliminate  $j$  from the list  $\mathcal{C}$ 
12:      continue
13:    end if
14:    if  $(r > \maxB(\mathcal{X}))$  OR  $(c\text{RMSD}(\mathcal{X}) > \maxC(\mathcal{X}))$  then
15:      continue
16:    end if
17:     $A \leftarrow J$ 
18:    insert match  $A$  into  $\mathbb{A}$ 
19:  end for
20: end for
21: return  $\mathbb{A}$ 

```

4.2 MODEL ARCHITECTURES

The model takes the antigen-antibody complex’s structure and sequence context, along with the sequences of the CDR-like fragments, as conditional inputs to iteratively denoise. The first branch of the model learns the global context information of the complex, while another branch takes the local homologous information of CDR-like fragments as input, aiming to learn the functional similarity and evolutionary information of residues with similar structure. The two branches are combined to generate the antibody CDR sequence jointly.

4.2.1 GLOBAL GEOMETRY CONTEXT INFORMATION BRANCH

Context encoder A protein is formed by the connection of multiple residues. The features of a single residue mainly include the residue type, backbone atom coordinates, and backbone dihedral angles. The features of each pair of residues mainly include the types of both residues, sequential relative position, spatial distance, and pairwise backbone dihedrals. These features are concatenated and then input into two separate MLPs. The output is denoted as z_i and y_{ij} .

Evolutionary encoder Recent advances have shown the structure-informed protein language model (PLM) is an excellent tool for creating protein sequence embeddings and providing evolutionary information (Zheng et al., 2023; Shanker et al., 2024). Thus, we take ESM2 (Lin et al., 2023) as an antibody sequence encoder, aiming to capture the evolutionary relations of antibody residues. The state of antibody sequence with CDR at timestep t is fed into it and output is defined as e^t .

Structure-informed network The above encoding is used as conditional input to the Structure-informed network. They, along with the CDR sequence and structural state at the current time step, will be input into a stack of Invariant Point Attention (IPA) (Jumper et al., 2021) layers, and jointly transform into a hidden representation h_i . Subsequently, the hidden representation h_i is transformed by an MLP to obtain the probability representation r_{global} of the amino acid type at each CDR site. This probability representation is then input to the local CDR-focused branch.

4.2.2 LOCAL CDR-FOCUSED INFORMATION BRANCH

Post-processing of CDR-like fragments We first remove the CDR portions from the antibody sequences to obtain the antibody framework sequences. Then, we fill these fragments’ short sequences into the antibody framework sequences, thereby constructing a CDR-like sequence matrix \mathbf{E} .

CDR-focused Axial Attention The local CDR-like branch is constituted of a stack of axial attention layers, referred to as CDR-focused Axial Attention. Given that the CDR-like fragments exhibit structures similar to actual CDRs, we employed a tied row attention mechanism used in MSATransformer (Rao et al., 2021) to leverage these retrieval results. In the standard axial attention (Ho et al., 2019) mechanism, each row and column are considered independently. However, in MSA (Multiple Sequence Alignment), each sequence exhibits relatively similar structural features. Our matrix format is well-suited for adopting a tied row attention mechanism to fully utilize the structural similarity. When calculating the attention scores for each row, this mechanism simultaneously considers the scores of other rows. This approach not only leverages the structural similarity but also reduces memory usage.

The input to CDR-focused Axial Attention is a pseudo-MSA matrix \mathbf{P} in equation 3. The first row of this matrix is initially filled with the antigen-antibody framework sequence, with the CDR region populated by the noisy sequence R_g^t (sampled by r_{global}) at the current time step t . From the second row to the k -th row (where k is chosen to be 16, meaning the top 15 retrieved CDR-like sequences are used as conditional input), the rows are filled with the CDR-like sequence matrix \mathbf{E} . The constructed matrix \mathbf{P} is then input to CDR-focused Axial Attention to create the homologous embedding and calculate the probability representation r_{local} (equation 4).

$$\mathbf{P} = \text{concat} \left((S_{ab} \cup R_g^t), \mathbf{E} \right) \quad (3)$$

$$\begin{aligned} r_{\text{local}}[\cdot, j] &= G_{\text{col}}(\mathbf{P}_{\cdot, j}, t) \text{ for all } j \in \text{col}, \\ r_{\text{local}}[i, \cdot] &= G_{\text{tiedrow}}(\mathbf{P}_{i, \cdot}, t) \text{ for all } i \in \text{row} \end{aligned} \quad (4)$$

The row self-attention is computed to capture the internal relationships within the antibody-antigen sequences, while the column self-attention is computed to capture the relationships between the CDR residues and the CDR-like residues.

Skip connection for information fusion Although the probability distribution of the CDR region created by the antigen-antibody context features has already been fed into the network, to prevent the loss of antigen-antibody context information during forward propagation, the embedding r_{local} and r_{global} are added by a skip connection module (He et al., 2016), then execute *softmax* to obtain the final probability distribution.

4.3 MODEL TRAINING AND INFERENCE

The overall training objective The training objective is to minimize the probability distributions predicted by the network under two conditions at each time step and the true posterior distribution at the same time step. Therefore, we choose KL divergence between the two distributions at each residue in the CDR region as the training loss function,

$$L_{\text{type}}^t = \mathbb{E}_{\mathcal{R}^t \sim p} \left[\frac{1}{m} \sum_j D_{\text{KL}} \left(q(s_j^{t-1} | s_j^t, s_j^0) || p(s_j^{t-1} | \mathcal{R}^t, C_{ab}, C_{ag}, \mathbb{A}) \right) \right] \quad (5)$$

The training objective of the whole diffusion process is:

$$L = E_{t \sim \text{Uniform}(1..T)} L_{\text{type}}^t \quad (6)$$

Conditional reverse diffusion process We employ DDPM to generate sequences. The model starts from time step T , initializing each site of the antibody CDR region as a uniform distribution. Then, through the frozen ESM encoder $E(\cdot)$, learned global context network $F(\cdot)[j]$ and the local CDR-focused network $G(\cdot)[j]$, they predict the noise distribution at each time step jointly and denoise step-by-step:

$$e^t = E(S_{ab} \cup R^t) \quad (7)$$

Table 1: Results of sequence design on SAbDab dataset

Method	CDR-H1			CDR-H2			CDR-H3		
	AAR(%) \uparrow	scRMSD \downarrow	Plausibility \uparrow	AAR(%) \uparrow	scRMSD \downarrow	plausibility \uparrow	AAR(%) \uparrow	scRMSD \downarrow	plausibility \uparrow
Grafting	58.05	0.83	-0.597	31.46	0.79	-0.619	19.63	3.20	-0.591
ProteinMPNN	58.58	0.64	-0.603	53.18	0.61	-0.568	41.77	2.27	-0.605
ESM-IF1	53.80	0.66	-0.610	46.66	0.63	-0.589	29.82	2.59	-0.607
Diffab-fix	74.93	0.66	-0.512	65.41	0.59	-0.532	49.17	2.24	-0.541
AbMPNN*	72.83	1.09	-0.664	65.33	0.93	-0.677	52.99	2.80	-0.675
RADAb	76.57	0.61	-0.505	66.16	0.57	-0.530	57.02	2.23	-0.530

Method	CDR-L1			CDR-L2			CDR-L3		
	AAR(%) \uparrow	scRMSD \downarrow	Plausibility \uparrow	AAR(%) \uparrow	scRMSD \downarrow	plausibility \uparrow	AAR(%) \uparrow	scRMSD \downarrow	plausibility \uparrow
Grafting	68.53	0.85	-0.506	43.19	0.52	-0.573	43.61	1.08	-0.395
ProteinMPNN	45.60	0.59	-0.612	46.78	0.46	-0.527	47.21	0.98	-0.543
ESM-IF1	40.97	0.61	-0.650	43.40	0.43	-0.542	38.93	0.92	-0.569
Diffab-fix	79.78	0.56	-0.386	81.19	0.44	-0.398	67.97	0.88	-0.414
AbMPNN*	75.06	0.73	-0.543	71.63	0.56	-0.528	64.51	0.91	-0.544
RADAb	83.72	0.54	-0.379	84.58	0.44	-0.384	73.11	0.87	-0.384

$$p(s_j^{t-1} | \mathcal{R}^t, \mathcal{C}_{ab}, \mathcal{C}_{ag}, \mathbb{A}) = \text{Multinomial} [F(\mathcal{R}^t, \mathcal{C}_{ab}, \mathcal{C}_{ag}, e^t) + G(F(\mathcal{R}^t, \mathcal{C}_{ab}, \mathcal{C}_{ag}, e^t), \mathbb{A})] [j] \quad (8)$$

During sampling, we remove the CDR region sequences from the antibody structures and fill them with noisy sequence sampled from the uniform distribution. The retrieval process uses the structure of the CDR region as input and outputs a set of CDR-like fragments. Subsequently, this set of CDR-like fragments is fed into the retrieval-augmented diffusion model, serving as a condition along with the antigen-antibody framework context to guide the model in step-by-step denoising and generating the CDR sequences.

5 EXPERIMENTS

To evaluate the performance of our model’s generation, we utilize two tasks: antibody CDR sequence inverse folding (Section 5.1) and antibody optimization based on sequence design (Section 5.2), to compare with the baselines. Additionally, we conducted ablation experiments and further analysis to demonstrate the effectiveness of the retrieval-augmented method (Section 5.3).

The dataset for training the model is obtained from the SAbDab and our established CDR-like fragments dataset. Following the previous work (Luo et al., 2022), we first eliminated structures with a resolution lower than 4Å and removed antibodies that target non-protein antigens. Chothia (Chothia & Lesk, 1987) in ANARCI (Dunbar & Deane, 2016) is used for renumbering antibody residues. We clustered the SAbDab datasets based on 50% sequence similarity in the CDR-H3 region, and chose 50 PDB files comprising 63 antibody-antigen complex structures as the test set. To ensure distinct training and test sets, we removed structures from the training set that were part of the same clusters as those in the test set.

5.1 ANTIBODY CDR SEQUENCE INVERSE FOLDING

Baselines For traditional methods, we simulated a method of grafting using CDR-like data in the process of rational antibody design. Specifically, we directly graft the retrieved top-1 CDR-like fragment onto the antibody framework, termed **Grafting**. For deep learning methods, we selected a series of state-of-the-art protein inverse folding models for comparison with our work, including **ProteinMPNN** (Dauparas et al., 2022), a model that utilizes message passing neural network to design sequences with a fixed protein backbone; **ESM-IF** (Hsu et al., 2022), a protein inverse folding model that trained on millions of predicted structures; **Diffab-fix** (Luo et al., 2022), which can fix the backbone structure and iteratively generate candidate sequences from pure noise in sequence space using diffusion; **AbMPNN** (Dreyer et al., 2023), a model fine-tuned ProteinMPNN on antibody sequence and structure. Because it is not open-sourced, we evaluate it on its own test set. For more baseline details, please refer to Appendix A.5.

Metrics To evaluate the accuracy and rationality of the sequences generated by the model, we selected the following three popular evaluation metrics: (1) Amino Acid Recovery (AAR,%): AAR refers to the ratio of positions where the designed sequence and the true CDR sequence have the same amino acid; (2) Self-consistency RMSD (scRMSD, Å): To calculate scRMSD, we refold the antibody sequences generated by the model using ABodyBuilder2 (Abanades et al., 2023). Then, we

Table 2: Results of long CDRH3 sequence design performance.

Method	AAR(%)	scRMSD	plausibility
Grafting	7.79	4.05	-0.785
ProteinMPNN	46.63	2.71	-0.820
ESM-IF1	30.01	2.86	-0.845
Diffab-fix	42.26	3.02	-0.740
AbMPNN*	43.27	4.39	-1.012
RADAb	51.35	2.52	-0.747

Table 3: Results of binding energy optimization based on antibody sequence design.

Method	$\Delta\Delta G\downarrow$	$\Delta\Delta G\text{-seq}\downarrow$	IMP-seq(%) \uparrow
Grafting	135.17	40.22	32.69
ProteinMPNN	127.14	24.72	35.51
ESM-IF1	162.09	42.28	33.33
Diffab-fix	116.36	14.05	34.52
RADAb	109.16	7.06	37.30

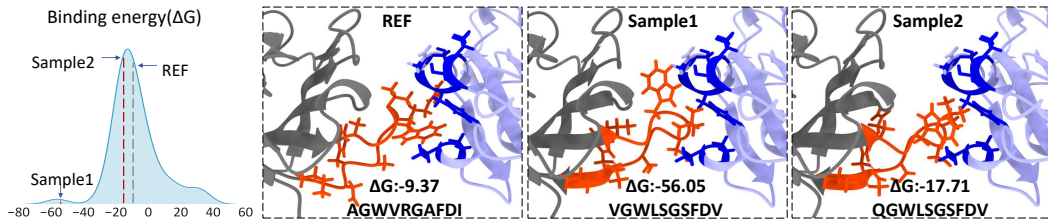


Figure 3: Left: Distribution of the samples' interface energy. Right: Generated CDR-H3 samples and the original structure of PDB: 7d61 antigen-antibody complex. The gray part represents the antibody framework, the red part represents the CDR, and the blue part represents the antigen (with the darker shade indicating the antigen epitope).

align the refolded antibody framework with the original antibody and compute the RMSD of the C_α atoms in the CDR region. (3) Plausibility: We use pseudo-log-likelihood in an antibody language model, AntiBERTy (Ruffolo et al., 2021) to calculate plausibility of the generated sequence.

Results As shown in Table 1, RADAb outperforms state-of-the-art methods in each metric and at each CDR region. In particular, in the highly variable and specific CDR-H3 region (Shirai et al., 1999; Raybould et al., 2019), our method achieved a great improvement in AAR compared to best-performing methods Diffab-fix and AbMPNN. The evaluation results indicate that the retrieval-augmented method, by introducing structurally similar homologous sequences, has improved the accuracy, consistency, and rationality of the model's generation.

In addition, CDR-H3 exhibits significant variability in length, sequence, and structure. Typically, deep learning models show decreased performance when generating longer CDR-H3 sequences (Luo et al., 2022; Høie et al., 2024). Therefore, we selected a subset of the test set with CDR-H3 lengths longer than 14 to evaluate the generation performance. As shown in Table 2, while the generation performance of all methods declines to some extent, our method demonstrates consistency and significantly outperforms the others, with a larger margin of improvement.

5.2 ANTIBODY FUNCTIONALITY OPTIMIZATION

In this section, we focus on the evolution of antibody sequences and evaluate whether the structure of the evolved sequence has greater functionality compared to the structure of the folded original sequence. To this end, we first fold the designed CDR-H3 sequences with framework sequences and the original real antibody sequences into complete protein structures using ABodyBuilder2. Then, we use *FastRelax* and *InterfaceAnalyzer* in PyRosetta (Alford et al., 2017) to relax the structure and calculate the binding energy ΔG of the antibody-antigen complex.

Metrics We use various metrics to evaluate the efficacy and functionality of our designed antibodies: (1) $\Delta\Delta G$: This metric represents the difference in binding energy between the complex with the designed CDR folded into the structure and the original complex binding energy. (2) $\Delta\Delta G\text{-seq}$: This metric measures the difference in binding energy between the complex with the designed CDR sequence folded into the structure and the binding energy of the original antibody sequence folded into the structure. It aims to eliminate errors introduced by the folding tool, allowing for a direct comparison of sequence functionality. (3) IMP-seq: This metric indicates the percentage of designed

Table 4: Ablation Study. G represents using Ground truth as retrieval results, R represents the Retrieval-augment mechanism, and E represents Evolutionary embedding mechanism.

G	Ablation			AAR(%)	scRMSD	Plausibility
	R	E				
✓	✓	✓		70.56	2.13	-0.534
✗	✗	✓		51.36	2.23	-0.538
✗	✓	✗		52.15	2.39	-0.529
✗	✗	✗		49.17	2.24	-0.541
✗	✓	✓		57.02	2.23	-0.530

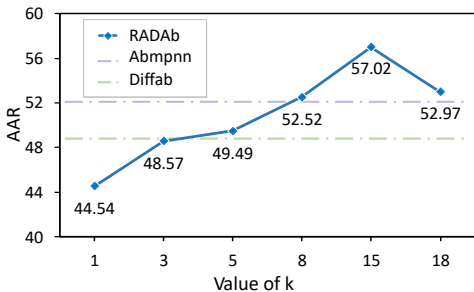


Figure 4: The effect of the value of CDR-like fragments k on model’s CDRH3 performance.

CDR sequences folded into the structure with a lower (better) binding energy than the original antibody sequences folded into the structure.

Results As shown in Table 3, after folding and relaxing, the antibody sequences we designed show a significant decrease in binding energy compared to other methods, and 37.3% of them have better binding energy than those folded from the original antibody sequences.

To further demonstrate the optimization of antibody sequence functionality by RADAb, we select a specific antigen-antibody complex from the test set (A neutralizing MAb targeting the receptor-binding domain of SARS-CoV-2, PDB: 7d6i). We generate 50 sequences for CDR-H3 and calculate the binding energy ΔG of the folded structures. Among these, 68% of the samples exhibited lower ΔG compared to the original complex. As shown in Figure 3, we select two samples as examples. Although they do not achieve the highest AAR, they demonstrate better binding affinity compared to the native structure.

5.3 ANALYSIS

Ablation We conducted a series of ablation experiments for CDR-H3 following the settings described in Section 5.1 to validate the effectiveness and relative contributions of the additional conditions and data we introduced. The specific objectives are: (1) to verify the effectiveness of the retrieval augment module; (2) to assess the validity of the retrieved data; and (3) to evaluate the effectiveness of the evolutionary embedding.

As shown in Table 4, We demonstrated the retrieval augment module’s effectiveness by inputting the CDR sequence’s ground truth into this module. We also removed the retrieval augmentation mechanism and the evolutionary embedding mechanism respectively to validate their effectiveness. The experimental results show that both the retrieval augmentation module and the evolutionary embedding module individually improve performance, and using them together maximizes the model’s performance.

Effect of retrieval dataset To further analyze the benefits brought by the retrieval mechanism and retrieved motifs, we conducted a series of comparative experiments on the value k of CDR-like fragments selected as conditions in the diffusion network, as shown in Figure 4. We found that when the value of k is low, it brings negative benefits to the model, which may be due to overfitting. As the value of k increases, the model performance also gradually improves. When k equals 15, the model achieves the best performance. But when k exceeds 15, the additional information instead introduces noise to the model, leading to performance degradation.

6 CONCLUSION AND FUTURE WORKS

In this work, we propose a retrieval-augmented diffusion generative model RADAb for antibody sequence design. This model leverages global geometric information and local template information, incorporating these conditions into the diffusion process to enhance antibody sequence design and optimization. Experimental results demonstrate that RADAb achieves state-of-the-art performance across multiple tasks. The main limitation of this work is that it has not yet been fully validated in wet lab experiments, which will be one of the major tasks in the future. Since we have proposed a

486 comparatively general retrieval method and retrieval-augment framework, another major future task
487 is to extend the model to the design of various protein motifs.

488 489 REPRODUCIBILITY STATEMENT

490 We provide the implementation details of our method and baselines in Appendix A. The code is
491 available at <https://anonymous.4open.science/r/RADAb-111F>.

492 493 REFERENCES

494 Brennan Abanades, Wing Ki Wong, Fergus Boyles, Guy Georges, Alexander Bujotzek, and Char-
495 lotte M Deane. Immunebuilder: Deep-learning models for predicting the structures of immune
496 proteins. *Communications Biology*, 6(1):575, 2023.

497 Jared Adolf-Bryfogle, Oleks Kalyuzhnyi, Michael Kubitz, Brian D Weitzner, Xiaozhen Hu, Yumiko
498 Adachi, William R Schief, and Roland L Dunbrack Jr. Rosettaantibodydesign (rabd): A general
499 framework for computational antibody design. *PLoS computational biology*, 14(4):e1006112,
500 2018.

501 Mauricio Aguilar Rangel, Alice Bedwell, Elisa Costanzi, Ross J Taylor, Rosaria Russo, Gonçalo JL
502 Bernardes, Stefano Ricagno, Judith Frydman, Michele Vendruscolo, and Pietro Sormanni.
503 Fragment-based computational design of antibodies targeting structured epitopes. *Science Ad-
504 vances*, 8(45):eabp9540, 2022.

505 Rahmad Akbar, Philippe A Robert, Milena Pavlović, Jeli azko R Jeli azkov, Igor Snapkov, Andrei
506 Slabodkin, Cédric R Weber, Lonneke Scheffer, Enkelejda Miho, Ingrid Hobæk Haff, et al. A
507 compact vocabulary of paratope-epitope interactions enables predictability of antibody-antigen
508 binding. *Cell Reports*, 34(11), 2021.

509 Bissan Al-Lazikani, Arthur M Lesk, and Cyrus Chothia. Standard conformations for the canonical
510 structures of immunoglobulins. *Journal of molecular biology*, 273(4):927–948, 1997.

511 Rebecca F Alford, Andrew Leaver-Fay, Jeli azko R Jeli azkov, Matthew J O’Meara, Frank P DiMaio,
512 Hahnbeom Park, Maxim V Shapovalov, P Douglas Renfrew, Vikram K Mulligan, Kalli Kappel,
513 et al. The rosetta all-atom energy function for macromolecular modeling and design. *Journal of
514 chemical theory and computation*, 13(6):3031–3048, 2017.

515 Helen M Berman, John Westbrook, Zukang Feng, Gary Gilliland, Talapady N Bhat, Helge Weissig,
516 Ilya N Shindyalov, and Philip E Bourne. The protein data bank. *Nucleic acids research*, 28(1):
517 235–242, 2000.

518 Andreas Blattmann, Robin Rombach, Kaan Oktay, Jonas Müller, and Björn Ommer. Retrieval-
519 augmented diffusion models. *Advances in Neural Information Processing Systems*, 35:15309–
520 15324, 2022.

521 Davide Caffagni, Federico Cocchi, Nicholas Moratelli, Sara Sarto, Marcella Cornia, Lorenzo
522 Baraldi, and Rita Cucchiara. Wiki-llava: Hierarchical retrieval-augmented generation for mul-
523 timodal llms. In *Proceedings of the IEEE/CVF Conference on Computer Vision and Pattern
524 Recognition*, pp. 1818–1826, 2024.

525 Cyrus Chothia and Arthur M Lesk. Canonical structures for the hypervariable regions of im-
526 munoglobulins. *Journal of molecular biology*, 196(4):901–917, 1987.

527 Justas Dauparas, Ivan Anishchenko, Nathaniel Bennett, Hua Bai, Robert J Ragotte, Lukas F Milles,
528 Basile IM Wicky, Alexis Courbet, Rob J de Haas, Neville Bethel, et al. Robust deep learning-
529 based protein sequence design using proteinmpnn. *Science*, 378(6615):49–56, 2022.

530 Frédéric A Dreyer, Daniel Cutting, Constantin Schneider, Henry Kenlay, and Charlotte M Deane. In-
531 verse folding for antibody sequence design using deep learning. *arXiv preprint arXiv:2310.19513*,
532 2023.

533 James Dunbar and Charlotte M Deane. Anarci: antigen receptor numbering and receptor classifica-
534 tion. *Bioinformatics*, 32(2):298–300, 2016.

- 540 James Dunbar, Konrad Krawczyk, Jinwoo Leem, Terry Baker, Angelika Fuchs, Guy Georges, Jiye
541 Shi, and Charlotte M Deane. Sabdad: the structural antibody database. *Nucleic acids research*,
542 42(D1):D1140–D1146, 2014.
- 543
544 Stefan Ewert, Annemarie Honegger, and Andreas Plückthun. Stability improvement of antibodies
545 for extracellular and intracellular applications: Cdr grafting to stable frameworks and structure-
546 based framework engineering. *Methods*, 34(2):184–199, 2004.
- 547 Nathan C Frey, Dan Berenberg, Karina Zadorozhny, Joseph Kleinhenz, Julien Lafrance-Vanasse,
548 Isidro Hotzel, Yan Wu, Stephen Ra, Richard Bonneau, Kyunghyun Cho, et al. Protein discovery
549 with discrete walk-jump sampling. In *The Twelfth International Conference on Learning Repre-*
550 *sentations*, 2023.
- 551 Pablo Gainza, Freyr Sverrisson, Frederico Monti, Emanuele Rodola, Davide Boscaini, Michael M
552 Bronstein, and Bruno E Correia. Deciphering interaction fingerprints from protein molecular
553 surfaces using geometric deep learning. *Nature Methods*, 17(2):184–192, 2020.
- 554
555 Pablo Gainza, Sarah Wehrle, Alexandra Van Hall-Beauvais, Anthony Marchand, Andreas Scheck,
556 Zander Hartevelde, Stephen Buckley, Dongchun Ni, Shuguang Tan, Freyr Sverrisson, et al. De
557 novo design of protein interactions with learned surface fingerprints. *Nature*, 617(7959):176–
558 184, 2023.
- 559 Yunfan Gao, Yun Xiong, Xinyu Gao, Kangxiang Jia, Jinliu Pan, Yuxi Bi, Yi Dai, Jiawei Sun, and
560 Haofen Wang. Retrieval-augmented generation for large language models: A survey. *arXiv*
561 *preprint arXiv:2312.10997*, 2023.
- 562
563 Kelvin Guu, Kenton Lee, Zora Tung, Panupong Pasupat, and Mingwei Chang. Retrieval augmented
564 language model pre-training. In Hal Daumé III and Aarti Singh (eds.), *Proceedings of the 37th*
565 *International Conference on Machine Learning*, volume 119 of *Proceedings of Machine Learning*
566 *Research*, pp. 3929–3938. PMLR, 13–18 Jul 2020.
- 567 Kaiming He, Xiangyu Zhang, Shaoqing Ren, and Jian Sun. Deep residual learning for image recog-
568 nition. In *Proceedings of the IEEE conference on computer vision and pattern recognition*, pp.
569 770–778, 2016.
- 570 Jonathan Ho, Nal Kalchbrenner, Dirk Weissenborn, and Tim Salimans. Axial attention in multidim-
571 ensional transformers. *arXiv preprint arXiv:1912.12180*, 2019.
- 572
573 Jonathan Ho, Ajay Jain, and Pieter Abbeel. Denoising diffusion probabilistic models. *Advances in*
574 *neural information processing systems*, 33:6840–6851, 2020.
- 575 Magnus Haraldson Høie, Alissa Hummer, Tobias H Olsen, Broncio Aguilar-Sanjuan, Morten
576 Nielsen, and Charlotte M Deane. Antifold: Improved antibody structure-based design using
577 inverse folding. *arXiv preprint arXiv:2405.03370*, 2024.
- 578
579 Emiel Hooeboom, Didrik Nielsen, Priyank Jaini, Patrick Forré, and Max Welling. Argmax flows
580 and multinomial diffusion: Learning categorical distributions. In M. Ranzato, A. Beygelzimer,
581 Y. Dauphin, P.S. Liang, and J. Wortman Vaughan (eds.), *Advances in Neural Information Pro-*
582 *cessing Systems*, volume 34, pp. 12454–12465. Curran Associates, Inc., 2021.
- 583
584 Chloe Hsu, Robert Verkuil, Jason Liu, Zeming Lin, Brian Hie, Tom Sercu, Adam Lerer, and Alexan-
585 der Rives. Learning inverse folding from millions of predicted structures. In *International con-*
586 *ference on machine learning*, pp. 8946–8970. PMLR, 2022.
- 587
588 Ziniu Hu, Ahmet Iscen, Chen Sun, Zirui Wang, Kai-Wei Chang, Yizhou Sun, Cordelia Schmid,
589 David A Ross, and Alireza Fathi. Reveal: Retrieval-augmented visual-language pre-training with
590 multi-source multimodal knowledge memory. In *Proceedings of the IEEE/CVF conference on*
591 *computer vision and pattern recognition*, pp. 23369–23379, 2023.
- 592
593 Zhilin Huang, Ling Yang, Xiangxin Zhou, Chujun Qin, Yijie Yu, Xiawu Zheng, Zikun Zhou, Wentao
Zhang, Yu Wang, and Wenming Yang. Interaction-based retrieval-augmented diffusion models
for protein-specific 3d molecule generation. In *Forty-first International Conference on Machine*
Learning, 2024.

- 594 Wengong Jin, Jeremy Wohlwend, Regina Barzilay, and Tommi S Jaakkola. Iterative refinement
595 graph neural network for antibody sequence-structure co-design. In *International Conference on*
596 *Learning Representations*, 2021.
- 597 Peter T Jones, Paul H Dear, Jefferson Foote, Michael S Neuberger, and Greg Winter. Replacing the
598 complementarity-determining regions in a human antibody with those from a mouse. *Nature*, 321
599 (6069):522–525, 1986.
- 600 John Jumper, Richard Evans, Alexander Pritzel, Tim Green, Michael Figurnov, Olaf Ronneberger,
601 Kathryn Tunyasuvunakool, Russ Bates, Augustin Žídek, Anna Potapenko, et al. Highly accurate
602 protein structure prediction with alphafold. *nature*, 596(7873):583–589, 2021.
- 603 Xiangzhe Kong, Wenbing Huang, and Yang Liu. Conditional antibody design as 3d equivariant
604 graph translation. In *The Eleventh International Conference on Learning Representations*, 2022.
- 605 Xiangzhe Kong, Wenbing Huang, and Yang Liu. End-to-end full-atom antibody design. In *Proceed-*
606 *ings of the 40th International Conference on Machine Learning*, pp. 17409–17429, 2023.
- 607 Paulina Kulytė, Francisco Vargas, Simon Valentin Mathis, Yu Guang Wang, José Miguel Hernández-
608 Lobato, and Pietro Liò. Improving antibody design with force-guided sampling in diffusion mod-
609 els, 2024.
- 610 Gideon D Lapidoth, Dror Baran, Gabriele M Pszolla, Christoffer Norn, Assaf Alon, Michael D
611 Tyka, and Sarel J Fleishman. Abdesign: A n algorithm for combinatorial backbone design guided
612 by natural conformations and sequences. *Proteins: Structure, Function, and Bioinformatics*, 83
613 (8):1385–1406, 2015.
- 614 Patrick Lewis, Ethan Perez, Aleksandra Piktus, Fabio Petroni, Vladimir Karpukhin, Naman Goyal,
615 Heinrich Küttler, Mike Lewis, Wen-tau Yih, Tim Rocktäschel, et al. Retrieval-augmented genera-
616 tion for knowledge-intensive nlp tasks. *Advances in Neural Information Processing Systems*, 33:
617 9459–9474, 2020.
- 618 Haitao Lin, Lirong Wu, Huang Yufei, Yunfan Liu, Odin Zhang, Yuanqing Zhou, Rui Sun, and Stan Z
619 Li. Geoab: Towards realistic antibody design and reliable affinity maturation. *bioRxiv*, pp. 2024–
620 05, 2024.
- 621 Zeming Lin, Halil Akin, Roshan Rao, Brian Hie, Zhongkai Zhu, Wenting Lu, Nikita Smetanin,
622 Robert Verkuil, Ori Kabeli, Yaniv Shmueli, et al. Evolutionary-scale prediction of atomic-level
623 protein structure with a language model. *Science*, 379(6637):1123–1130, 2023.
- 624 Alexander Long, Wei Yin, Thalaisyasingam Ajanthan, Vu Nguyen, Pulak Purkait, Ravi Garg, Alan
625 Blair, Chunhua Shen, and Anton van den Hengel. Retrieval augmented classification for long-tail
626 visual recognition. In *Proceedings of the IEEE/CVF conference on computer vision and pattern*
627 *recognition*, pp. 6959–6969, 2022.
- 628 Shitong Luo, Yufeng Su, Xingang Peng, Sheng Wang, Jian Peng, and Jianzhu Ma. Antigen-specific
629 antibody design and optimization with diffusion-based generative models for protein structures.
630 *Advances in Neural Information Processing Systems*, 35:9754–9767, 2022.
- 631 Karolis Martinkus, Jan Ludwiczak, Wei-Ching Liang, Julien Lafrance-Vanasse, Isidro Hotzel,
632 Arvind Rajpal, Yan Wu, Kyunghyun Cho, Richard Bonneau, Vladimir Gligorijevic, et al. Ab-
633 diffuser: full-atom generation of in-vitro functioning antibodies. *Advances in Neural Information*
634 *Processing Systems*, 36, 2024.
- 635 Tobias H Olsen, Iain H Moal, and Charlotte M Deane. Ablang: an antibody language model for
636 completing antibody sequences. *Bioinformatics Advances*, 2(1):vbac046, 2022.
- 637 Leonard G Presta. Antibody engineering. *Current Opinion in Structural Biology*, 2(4):593–596,
638 1992.
- 639 Jiahua Rao, Zifei Shan, Longpo Liu, Yao Zhou, and Yuedong Yang. Retrieval-based knowledge aug-
640 mented vision language pre-training. In *Proceedings of the 31st ACM International Conference*
641 *on Multimedia*, pp. 5399–5409, 2023.

- 648 Roshan M Rao, Jason Liu, Robert Verkuil, Joshua Meier, John Canny, Pieter Abbeel, Tom Sercu,
649 and Alexander Rives. Msa transformer. In *International Conference on Machine Learning*, pp.
650 8844–8856. PMLR, 2021.
- 651
- 652 Matthew IJ Raybould, Claire Marks, Konrad Krawczyk, Bruck Taddese, Jaroslaw Nowak, Alan P
653 Lewis, Alexander Bujotzek, Jiye Shi, and Charlotte M Deane. Five computational developability
654 guidelines for therapeutic antibody profiling. *Proceedings of the National Academy of Sciences*,
655 116(10):4025–4030, 2019.
- 656 Jeffrey A Ruffolo, Jeffrey J Gray, and Jeremias Sulam. Deciphering antibody affinity maturation
657 with language models and weakly supervised learning. *arXiv preprint arXiv:2112.07782*, 2021.
- 658
- 659 Amir Shanehsazzadeh, Julian Alverio, George Kasun, Simon Levine, Jibrán A Khan, Chelsea
660 Chung, Nicolas Diaz, Breanna K Luton, Ysis Tarter, Cailen McCloskey, et al. In vitro validated
661 antibody design against multiple therapeutic antigens using generative inverse folding. *bioRxiv*,
662 pp. 2023–12, 2023a.
- 663 Amir Shanehsazzadeh, Sharrol Bachas, Matt McPartlon, George Kasun, John M Sutton, Andrea K
664 Steiger, Richard Shuai, Christa Kohnert, Goran Rakocevic, Jahir M Gutierrez, et al. Unlocking
665 de novo antibody design with generative artificial intelligence. *bioRxiv*, pp. 2023–01, 2023b.
- 666
- 667 Varun R Shanker, Theodora UJ Bruun, Brian L Hie, and Peter S Kim. Unsupervised evolution of
668 protein and antibody complexes with a structure-informed language model. *Science*, 385(6704):
669 46–53, 2024.
- 670
- 671 Shelly Sheynin, Oron Ashual, Adam Polyak, Uriel Singer, Oran Gafni, Eliya Nachmani, and Yaniv
672 Taigman. knn-diffusion: Image generation via large-scale retrieval. In *The Eleventh International
673 Conference on Learning Representations*, 2023.
- 674 Hiroki Shirai, Akinori Kidera, and Haruki Nakamura. H3-rules: identification of cdr-h3 structures
675 in antibodies. *FEBS letters*, 455(1-2):188–197, 1999.
- 676
- 677 Jascha Sohl-Dickstein, Eric Weiss, Niru Maheswaranathan, and Surya Ganguli. Deep unsupervised
678 learning using nonequilibrium thermodynamics. In *International conference on machine learn-
679 ing*, pp. 2256–2265. PMLR, 2015.
- 680 Jiaming Song, Chenlin Meng, and Stefano Ermon. Denoising diffusion implicit models. *arXiv
681 preprint arXiv:2010.02502*, 2020.
- 682
- 683 Pietro Sormanni, Francesco A Aprile, and Michele Vendruscolo. Rational design of antibodies
684 targeting specific epitopes within intrinsically disordered proteins. *Proceedings of the National
685 Academy of Sciences*, 112(32):9902–9907, 2015.
- 686
- 687 Amelia Villegas-Morcillo, Jana Weber, and Marcel Reinders. Guiding diffusion models for antibody
688 sequence and structure co-design with developability properties. In *NeurIPS 2023 Generative AI
689 and Biology (GenBio) Workshop*, 2023.
- 690 Danqing Wang, YE Fei, and Hao Zhou. On pre-training language model for antibody. In *The
691 eleventh international conference on learning representations*, 2023a.
- 692
- 693 Zichao Wang, Weili Nie, Zhuoran Qiao, Chaowei Xiao, Richard Baraniuk, and Anima Anandkumar.
694 Retrieval-based controllable molecule generation. In *The Eleventh International Conference on
695 Learning Representations*, 2023b.
- 696
- 697 Fang Wu and Stan Z. Li. A hierarchical training paradigm for antibody structure-sequence co-design.
698 In A. Oh, T. Naumann, A. Globerson, K. Saenko, M. Hardt, and S. Levine (eds.), *Advances in
699 Neural Information Processing Systems*, volume 36, pp. 31140–31157. Curran Associates, Inc.,
700 2023.
- 701 John L Xu and Mark M Davis. Diversity in the cdr3 region of vh is sufficient for most antibody
specificities. *Immunity*, 13(1):37–45, 2000.

702 Peng Xu, Wei Ping, Xianchao Wu, Lawrence McAfee, Chen Zhu, Zihan Liu, Sandeep Subramanian,
703 Evelina Bakhturina, Mohammad Shoeybi, and Bryan Catanzaro. Retrieval meets long context
704 large language models. In *The Twelfth International Conference on Learning Representations*,
705 2024.

706 Ori Yoran, Tomer Wolfson, Ori Ram, and Jonathan Berant. Making retrieval-augmented language
707 models robust to irrelevant context. In *The Twelfth International Conference on Learning Repr-*
708 *esentations*, 2024.

709 Mingyuan Zhang, Xinying Guo, Liang Pan, Zhongang Cai, Fangzhou Hong, Huirong Li, Lei Yang,
710 and Ziwei Liu. Remodiffuse: Retrieval-augmented motion diffusion model. In *Proceedings of*
711 *the IEEE/CVF International Conference on Computer Vision*, pp. 364–373, 2023a.

712 Peitian Zhang, Shitao Xiao, Zheng Liu, Zhicheng Dou, and Jian-Yun Nie. Retrieve anything to
713 augment large language models. *arXiv preprint arXiv:2310.07554*, 2023b.

714 Zaixiang Zheng, Yifan Deng, Dongyu Xue, Yi Zhou, Fei Ye, and Quanquan Gu. Structure-informed
715 language models are protein designers. In *International conference on machine learning*, pp.
716 42317–42338. PMLR, 2023.

717 Jianfu Zhou and Gevorg Grigoryan. Rapid search for tertiary fragments reveals protein sequence–
718 structure relationships. *Protein Science*, 24(4):508–524, 2015.

719 Xiangxin Zhou, Dongyu Xue, Ruizhe Chen, Zaixiang Zheng, Liang Wang, and Quanquan Gu.
720 Antigen-specific antibody design via direct energy-based preference optimization. *arXiv preprint*
721 *arXiv:2403.16576*, 2024.

722 Tian Zhu, Milong Ren, and Haicang Zhang. Antibody design using a score-based diffusion model
723 guided by evolutionary, physical and geometric constraints. In *Forty-first International Confer-*
724 *ence on Machine Learning*, 2024.

725
726
727
728
729
730
731
732
733
734
735
736
737
738
739
740
741
742
743
744
745
746
747
748
749
750
751
752
753
754
755

A ADDITIONAL DETAILS

A.1 MODEL DETAILS

For feature dimensions, we set the single residue feature dimension to 128 and the pair feature dimension to 64. We leverage 6 IPA layers to capture geometry information. ESM2 650M is utilized in our model to create the embedding of antibody sequences, and the embedding dimension is 1280. In the local CDR-focus network, two layers of axial attention were used (two tied row self-attention and two column self-attention). The embedding dimension is 384, the hidden dimension is 1536, and number of attention heads is 6.

A.2 IMPLEMENTATION DETAILS

Our model was developed and executed within the PyTorch framework. For training, We chose the Adam optimizer with a learning rate of 0.0001, weight decay of 0.0, and momentum parameters beta1 and beta2 set to 0.9 and 0.999, respectively. To dynamically adjust the learning rate, we employed plateau as learning rate scheduler. When the validation loss plateaued, the learning rate was reduced by a factor of 0.8, with a minimum learning rate set to 5e-6. The scheduler’s patience was set to 10 epochs. The batch size is 8 during training. We design 8 samples for each CDR in the test set. All experiments are run on a single RTX4090 GPU, with a memory storage of 24GB.

Due to the high variability and specificity of the CDRH3 region, and it is considered the most critical part in determining antigen-antibody binding. We conducted separate training for the sequence design of this region, adding and removing noise only for the CDRH3 region in each training iteration, with a total of 100,000 iterations. The other five regions, being more conserved, were trained together for a total of 250,000 iterations (approximately equivalent to 50,000 iterations per region). The reverse generation process time step t is set to 100.

A.3 IMPLEMENTATION OF STRUCTURAL RETRIEVAL

The input consists of the backbone atom coordinates of each amino acid in the CDR region, forming a set of coordinate points \mathcal{X} . \mathbb{T} represents the structures of all proteins in the PDB database. \mathbb{A} represents a set of protein fragments representing CDR-like fragments corresponding to the input CDR structure. \mathcal{C} represents the set of fragments of each structure with a length of m . J represents a linear motif centered on residue j in the structure, with a length equal to the query fragment.

Assume that the coordinates of residue j are aligned with the central residue of \mathcal{X} , and then compute the RMSD of \mathcal{X} when aligned onto τ . If the input contains discontinuous multiple structures, cRMSD will be the cumulative RMSD of these structures. MaxA, maxB, and maxC are three different upper-bound thresholds. These thresholds are selected to improve the speed and accuracy of the retrieval algorithm (For detailed proof, please refer to MASTER (Zhou & Grigoryan, 2015)).

A.4 IMPLEMENTATION OF CDR-LIKE DATABASE CONSTRUCTING

To eliminate the computational overhead caused by structural retrieval during the model’s training and inferencing, we followed previous work (Aguilar Rangel et al., 2022) and initially executed the retrieval algorithm on all CDR structures of all antibodies to construct a CDR-like database.

Each of the CDR structures is used as a query to search for structurally similar motifs in the PDB database. The MASTER algorithm is used to match all CDRs against the entire PDB database to find CDR-like structures. This structural search is based on the Kabsch algorithm, using the RMSD of the $C\alpha$ coordinates. For CDR fragments of length 4, the RMSD threshold is 0.4, and the threshold is increased by 0.05 Å for each additional residue (with a maximum threshold set to 1.0 Å). In this way, we obtain a CDR-like fragments database corresponding to all CDR structures. Except for strictly filtering out results identical to real CDR sequences, no CDR sequence information was leaked in this process.

810 A.5 BASELINE DETAILS

811 A.5.1 TRADITIONAL METHODS

812 **Rosetta-Fixbb** (Adolf-Bryfogle et al., 2018) Rosetta-Fixbb can use energy functions for antibody
813 CDR sequence design. Since DiffAb has already been proven to outperform it (Luo et al., 2022; Wu
814 & Li, 2023) on sequence design task, we did not conduct additional comparisons.
815

816 **Grafting** To simulate the rational design commonly used in traditional antibody design methods,
817 which often involves grafting CDR loops. For each CDR region, we directly selected the top-1 frag-
818 ment(best) from the retrieval database for the structures in the test set and replaced the corresponding
819 original CDR loop sequences with it.
820

821 A.5.2 DEEP LEARNING METHODS

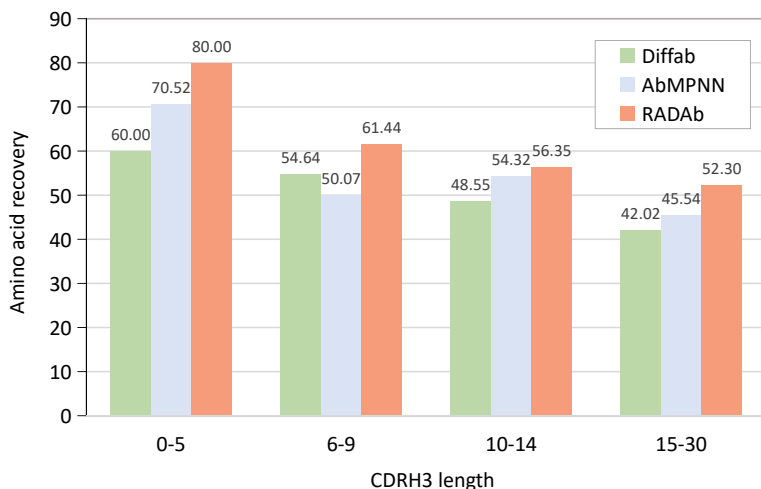
822 **ProteinMPNN** (Dauparas et al., 2022) ProteinMPNN is a deep learning framework for protein se-
823 quence inverse folding. It leverages a message passing neural network to model the complex rela-
824 tionships between amino acids in a protein structure. We use the antibody’s backbone structure as
825 input and keep the sequences outside the CDR regions to be designed fixed. We design sequences
826 for each CDR region separately. The sampling temperature is set to the default value of 0.1.
827

828 **Esm-IF1** (Hsu et al., 2022) Esm-IF1 is a protein sequence inverse folding model trained on millions
829 of AlphaFold2 predicted structures. We use the antibody’s backbone structure as input and keep the
830 sequences outside the CDR regions to be designed fixed. We design sequences for each CDR region
831 separately. The sampling temperature is set to the value of 0.2.
832

833 **Diffab-fix** (Luo et al., 2022) Diffab is a diffusion model that can design sequences of CDR re-
834 gion with a fixed CDR backbone. It takes antigen-antibody framework context as condition to
835 design CDR sequence. For a fair comparison, we retrained it with the default training configuration
836 *fixbb.yml*.

837 **AbMPNN** (Dreyer et al., 2023) AbMPNN is fine-tuned by antibody structure data and predicted
838 OAS (Observed Antibody Space) structure data. Its model architecture is consistent with Protein-
839 MPNN but achieves better performance in antibody inverse folding. We use the antibody’s backbone
840 structure as input and keep the sequences outside the CDR regions to be designed fixed. However,
841 it is not open-sourced yet, so we evaluate it on its own test set. We design sequences for each CDR
842 region separately. The sampling temperature is set to the default value of 0.1.
843

844 A.6 EXPERIMENT ON CDR-H3’S LENGTH



845
846
847
848
849
850
851
852
853
854
855
856
857
858
859
860
861
862
863
Figure S1: AAR distribution of different CDRH3 length

We further evaluated each model’s AAR across different CDR-H3 lengths. As shown in Figure S1, although the performance of all models decreases with increasing H3 length, our method still outperforms the others.

B STRUCTURE RECONSTRUCTION

To reconstruct the antibody structure, we use ABodyBuilder2 (Abanades et al., 2023), a deep learning model capable of predicting antibody light chain-heavy chain complexes. It is significantly faster than AlphaFold2 and offers higher prediction accuracy. We insert the designed CDR sequences into the antibody framework sequence, input it into ABodyBuilder2 to fold, and use OpenMM relax to obtain the structure corresponding to the new CDR sequences. Subsequently, we align the structure to the real antibody framework. Finally, we use the *fastrelax* function in PyRosetta (Alford et al., 2017), with the score function set to *ref2015* and max iteration set to 1000, to relax the structure.

C TRAINING AND INFERENCE ALGORITHM

In this section, we provide a detailed algorithm for the training (Algorithm 2) and inferencing (Algorithm 3) processes.

C.1 TRAINING ALGORITHM

Algorithm 2 Training Procedure of RADAb

```

1: Coordinates set  $\mathcal{X} = \{x_k \mid k \in \{1, \dots, m\}\}$ 
2:  $\mathbb{A} = \text{Retrieval}(\mathcal{X})$ 
3: while not convergence do
4:    $t \sim \text{Uniform}(1, \dots, T)$ 
5:    $q(s_j^{t-1} \mid s_j^t, s_j^0) = \frac{q(s_j^t \mid s_j^{t-1}) \cdot q(s_j^{t-1} \mid s_j^0)}{q(s_j^t \mid s_j^0)}$ 
6:    $S = S_{\text{fr}} \cup s_j^t$ 
7:    $e^t = E(S)$ 
8:   Context conditions  $\mathcal{C} \leftarrow \{\mathcal{R}^t, \mathcal{C}_{ab}, \mathcal{C}_{ag}\}$ 
9:    $p(s_j^{t-1} \mid \mathcal{C}, \mathbb{A}) = \text{Multinomial}[F(\mathcal{C}, e^t) + G(F(\mathcal{C}, e^t), \mathbb{A})][j]$ 
10:   $L_{\text{type}}^t = \mathbb{E}_{\mathcal{R}^t \sim p} \left[ \frac{1}{m} \sum_j D_{\text{KL}}(q(s_j^{t-1} \mid s_j^t, s_j^0) \parallel p(s_j^{t-1} \mid \mathcal{C}, \mathbb{A})) \right]$ 
11:   $F(\mathcal{C}, e^t), G(F(\mathcal{C}, e^t), \mathbb{A}) \leftarrow \text{Adam}(L_{\text{type}}^t)$ 
12: end while
13: return  $F(\cdot), G(\cdot)$ 

```

C.2 SAMPLING ALGORITHM

Algorithm 3 Sampling Procedure of RADAb

```

1:  $s_j^T \sim \text{Uniform}(20)$ 
2: Backbone coordinates set  $\mathcal{X} = \{x_k \mid k \in \{1, \dots, m\}\}$ 
3:  $\mathbb{A} = \text{Retrieval}(\mathcal{X})$ 
4: for  $t = T$  to 1 do
5:    $S = S_{\text{fr}} \cup s_j^t$ 
6:    $e^t = E(S)$ 
7:   Context conditions  $\mathcal{C} \leftarrow \{\mathcal{R}^t, \mathcal{C}_{ab}, \mathcal{C}_{ag}\}$ 
8:    $p(s_j^{t-1}) = \text{Multinomial}[F(\mathcal{C}, e^t) + G(F(\mathcal{C}, e^t), \mathbb{A})]$ 
9:   sample  $s_j^{t-1}$  from  $p(s_j^{t-1})$ 
10:   $R^{t-1} = \{s_j^{t-1} \mid j \in (a+1, \dots, a+m)\}$ 
11: end for
12: return  $R^0$ 

```

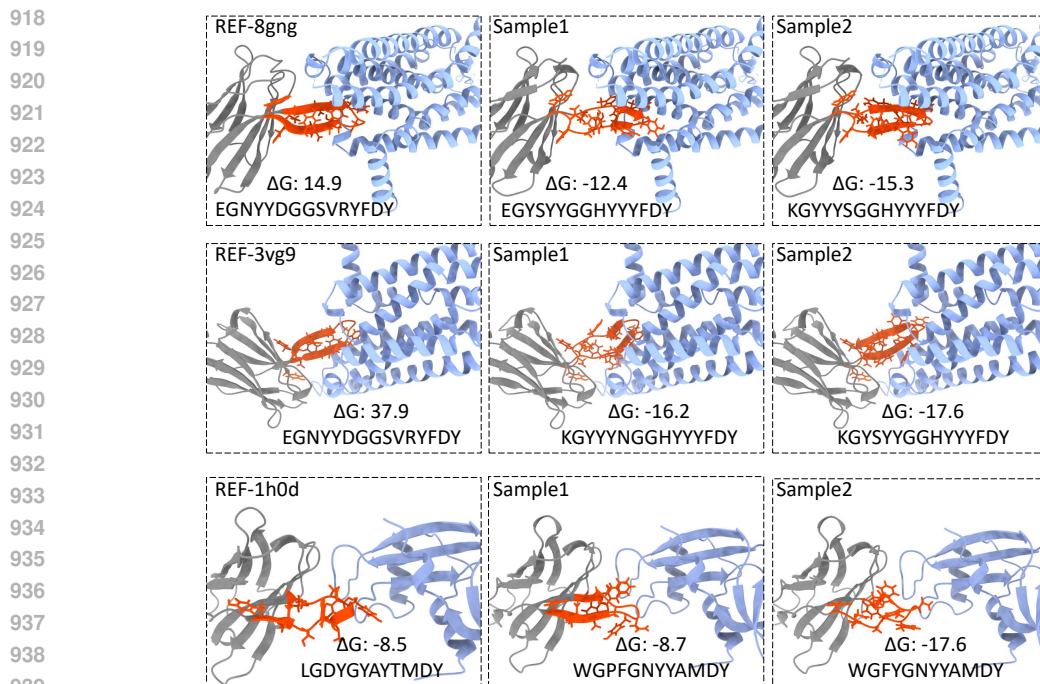


Figure S2: Optimized antibodies with lower binding energy. The gray parts represent the antibody framework, the red parts indicate the designed CDR regions, and the blue parts represent the antigen.

D CASE STUDY

We select a portion of the optimized antibodies in Figure S2. They achieved lower binding energy compared to the original antibody structures.

E THE REASON FOR ONLY CONSIDERING SEQUENCE DESIGN

Based on our observations, inverse folding represents a more practical scenario. Current structure-sequence co-design methods typically involve masking the CDR while retaining the presence of an antibody framework backbone, which represents a relatively uncommon use case. In most practical scenarios, we either have access to the full complex structure of the template antibody and the antigen, allowing us to perform inverse folding, or we lack a template molecule entirely, necessitating full atom and *de novo* design. This is also why researches from pharmaceutical companies and efforts involving in vitro experiments on antibody loop regions tend to focus more on designing antibodies through inverse folding, as evidenced by several recent studies (Shanehsazzadeh et al., 2023a;b; Frey et al., 2023; Høie et al., 2024; Shanker et al., 2024). This rationale underpins our decision to concentrate solely on this aspect in our work.

Another reason is that performing sequence-structure co-design while adhering to our retrieval-based approach would risk data leakage. This is because our retrieval process relies on the known structure of the CDR region, which is only possible when the CDR backbone is already known. At the same time, we recognize that epitope-specific full antibody *de novo* design, including full-atom design, is highly valuable. We are actively developing retrieval systems for PPI (Protein-Protein Interaction) retrieval to avoid potential data leakage and enhance our model.

Method	$\Delta\Delta G\downarrow$	$\Delta\Delta G\text{-seq}\downarrow$	IMP-seq(%) \uparrow	F-top1 \downarrow	F-top2 \downarrow	F-top3 \downarrow
Grafting	135.17	40.22	32.69	-	-	-
ProteinMPNN	127.14	24.72	35.51	-54.63	-45.58	-35.70
ESM-IF1	162.09	42.28	33.33	-62.65	-48.81	-33.86
Diffab-fix	116.36	14.05	34.52	-62.51	-54.80	-46.13
RADAb	109.16	7.06	37.30	-69.30	-55.95	-45.96

Table 5: Detailed results of antibody functionality optimization, F means functionality, which refers to $\Delta\Delta G\text{-seq}$

F DETAILED RESULTS OF ANTIBODY FUNCTIONALITY OPTIMIZATION

To further evaluate the model’s performance in optimizing antibody functionality, we additionally assessed the $\Delta\Delta G_{seq}$ of the top-1 to top-3 structures generated by the model. The results are shown in Table 5, which further demonstrate that the antibodies optimized by our model exhibit improved functionality.

G LIMITATIONS

Due to the inherent limitations of the MASTER algorithms, the retrieved linear motifs may have structural issues. Despite careful screening and filtering, a tiny portion of the data might have lengths that differ from the original CDR loops or may even become discontinuous due to missing residues. These exceptional cases may have a negative impact on our model. We hope that advances in structural retrieval and improvements in alignment will jointly address this issue.

When constructing the CDR-like fragments database, searching the entire PDB database using all CDR structures from the SabDab database takes approximately 100 hours. Additionally, the ESM2 encoding used to capture antibody sequence evolution information and the axial attention focused on local CDR in the denoising network require more computational resources than typical diffusion methods.

It is important to note that applying current retrieval mechanism to structure and sequence co-design poses a significant risk of data leakage. Specifically, the retrieval process inherently relies on using the CDR structure information as a query, which practically transforms the task into one resembling inverse folding. However, one potential approach is to incorporate PPI (Protein-Protein Interaction) retrieval, and we are currently experimenting with MASIF (Gainza et al., 2020; 2023) for this purpose. This will be explored further as part of our future work.